arXiv:physics/0610064v2 [physics.flu-dyn] 21 Jun 2007

The flow generated by an active olfactory system of the red swamp crayfish

P. Denissenko[1], S. Lukaschuk[1], T. Breithaupt[2]

December 4, 2021

[1] Fluid Dynamics Laboratory, University of Hull, HU6 7RX, UK
[2] Department of Biology, University of Hull, HU6 7RX, UK

Summary

Crayfish are nocturnal animals that mainly rely on their chemoreceptors to locate food. On a crayfish scale chemical stimuli received from a distant source are dispersed by an ambient flow rather than molecular diffusion. When the flow is weak or absent, food search can be facilitated by currents generated by the animal itself. Crayfish employ their anterior fan organs to produce a variety of flow patterns. Here we study the flow generated by *Procambarus clarkii* in response to odour stimulation. We found that while searching for food the crayfish generates one or two outward jets. These jets create an inflow which draws odour to the crayfish's anterior chemoreceptors. We quantified velocity fields in the inflow region using Particle Image Velocimetry. The results show that the inflow velocity decreases proportionally to the inverse distance from the animal so that it takes about a minute for an odour plume to reach the animal's chemoreceptors from a distance of 10 cm. We compare the inflow generated by live crayfish with that produced by a mimicking device, a phantom. The phantom consisted of two

nozzles and an inlet providing two jets and a sink so that the overall mass flux was zero. The use of a phantom enabled us to analyze the inflow at various jet parameters. We showed that variation of the jets' directions and relative intensities allows changing the direction of odour attraction. These results provide a rationale for biomimetic robot design. We discuss sensitivity and efficiency of such a robot.

Key words: chemical sensing, crayfish, PIV flow measurement, biomimetics

Introduction

In an aquatic environment, vital information about the presence and location of food is provided by chemical stimuli. In contrast to visual and acoustic stimuli, chemicals are dispersed relatively slowly by molecular diffusion and the ambient flow. Molecular diffusion is relevant for orientation of microscopic organisms (Blackburn et al., 1998) being inefficient at providing olfactory information to animals at distances larger than a few millimetres (Dusenbery, 1992; Weissburg, 2000). That is why large aquatic animals such as crayfish rely on the information extracted from macroscopic odour plumes. These plumes form downstream of the odour source by advection and turbulent diffusion (Balkovsky and Shraiman, 2002).

Animals can orientate towards an odour source by following the mean direction of the flow carrying odour molecules (odour-gated rheotaxis) or by evaluating parameters of the turbulent odour plumes (Vickers, 2000; Weissburg, 2000). Lobsters, crabs and crayfish have been shown to navigate towards odour sources using a combination of these strategies (Atema, 1996; Moore and Grills, 1999; Weissburg and Derby, 1995; Grasso and Basil, 2002).

Animal orientation under still water conditions such as in ponds, lakes, caves, or during slack tide, is less studied. In aquatic environments with little or no ambient water movement, the flow created by an animal itself could help in odour acquisition and orientation. Understanding the active olfactory mechanisms of crayfish inhabiting stagnant waters requires consideration of the flow patterns created by an animal and the transport of odour stimulus to the chemoreceptors. This knowledge can be applied to the design of a robot searching for chemical sources under the stagnant water conditions.

Crustaceans are well known for their ability to create directed water cur-

rents by pumping and fanning appendages (Herberholz and Schmitz, 2001; Atema, 1985; Budd et al, 1979; Burrows and Willows, 1969; Brock, 1926). Different appendages can create distinct currents. For example gill currents ventilate the gills, abdominal swimmeret currents aid in locomotion, and currents created by the anterior fan organs have been suggested to be used for odour acquisition and chemical signalling (Breithaupt, 2001).

The fan organs of a crayfish consist of the flagellae of the three bilateral maxillipeds. As shown in Fig. 1A, fan organs are located below mouth and antennules, which constitute the major chemoreceptors in decapod crustaceans. The distal part of the multi-segmental flagella bears a dense single-layered array of feathered hairs emerging on either side of the stem (Fig. 1B). During a power stroke the hairs are erect, during a recovery stroke the hairs are tilted and the stem is flexed in order to reduce the drag (Fig. 1C). The fan organs can be used for chemical communication by generating a forward directed jet (Breithaupt and Eger, 2002, Bergman et al., 2005) or for odour acquisition by drawing water towards the head region (Breithaupt, 2001). In decapod crustaceans, odour stimulation generally initiates fanning activity (Atema, 1985; Brock, 1926). Crayfish with fan organs restrained were not able to find the odour source (Breithaupt, unpublished data).

The red swamp crayfish *Procambarus clarkii* inhabits rice fields and other stagnant water bodies and therefore might utilize fanning as an active olfactory mechanism. The mechanism by which the fan-generated currents draw water towards the olfactory appendages is not understood. Here we investigate how the red swamp crayfish uses outward directed currents to generate an inflow that could serve for odour acquisition. We visualized the jets generated by a crayfish and used Particle Image Velocimetry (PIV) to quantify the flow velocity around live animal.

In order to test a proposed mechanism for active odour acquisition we designed a phantom, an assembly of nozzles, simulating the flow pattern by producing the jets. The phantom enabled us to reproduce various velocity fields observed in crayfish. Behaviour of crustaceans has been used as the model for development of autonomous robots searching for chemical sources (Grasso, 2001; Ayers, 2004; Ishida et al., 2006; Martinez et al. 2006). Active generation of the flow might help to locate chemical sources in still fluids. Our phantom can be used as a prototype design of robots orienting by chemical clues.

Materials and methods

Flow visualization and PIV measurements were conducted for five adult animals: one female and four males of 7 to 8 cm body length. A crayfish was suspended with a holder glued to its back in an aquarium of the size of $60 \times 60 \times 120$ cm as shown in Fig. 2. A video camera (VC) was used to monitor activity of fan organs and position of antennules of the crayfish. The crayfish was suspended above a double wheeled freely rotating treadmill (TM) with the walking legs of each side resting on a separate wheel. The treadmill was aimed to reduce agitation of the animal. It helped the crayfish to rest or to perform natural walking movements involved in olfactory search behaviour. To prevent animals from reacting to visual disturbances they were blindfolded by wrapping an opaque tape around the eyestalks and the rostrum. The animal claws were removed by inducing autotomy since they interfere with flow measurements by shadowing the laser-sheet. Experiments with the unrestrained crayfish showed that claws are kept motionless during the odour acquisition so that their removal is not likely to affect the olfactory mechanism (Breithaupt, unpublished data).

We visualized the flow created by a crayfish by introducing water-based ink in proximity of its fan organs. As it will be discussed in details, the flow around the crayfish consists of the outward jets produced by fan organs and the inflow carrying the odour towards the animal's chemoreceptors. To measure the velocity field in the inflow area we used a two-dimensional PIV system (Dantec Dynamics, Ltd) including a 125 mJ double pulse Nd YAG laser and a Hi-Sense 12-bit double-frame CCD camera (Dantec) with the resolution 1280×1024 pixels. The FlowMap software (Dantec) was used to calculate the velocity field with the adaptive cross-correlation algorithm. Streamlines were calculated using MATLAB 7.0 software (The MathWorks). Silvered hollow glass spheres of diameter 10 μm and density 1.03 g/cm^3 were used as seeding particles. For PIV measurements of the horizontal velocity field the laser sheet and the camera were aligned at LS1 and C1 positions as shown in Fig. 2. For measurements in the vertical plane they were set at positions LS2 and C2. Both the laser source and the camera were fixed on a frame attached to a vertical translational stage which allows measurement of the velocity field at various distances from the bottom. A time interval between the laser pulses was set at 50 ms to measure the low magnitude velocity in the inflow area. With this time interval the higher velocity within outward jets could not be resolved. Flow measurements within the jets were not

attempted as the animal often changes the jet directions and these changes require re-alignment of the laser sheet and cameras.

After the crayfish was set to the measurement position, it was allowed to settle down for at least half an hour. After it started fanning, the PIV was triggered to acquire data at a rate of 1 frame per second. Only the images acquired during the 30 seconds of each experimental run were taken for analysis. Following these 30 seconds the animal often ceased waving its fan organs reacting to the laser pulses. It is likely that the crayfish retinal or the extra-retinal (Sandeman et al. 1990, Edwards, 1984) photoreceptors have been stimulated by the light scattered by the animal's translucent body.

To model the flow generating mechanism involved in chemoreception of the crayfish we designed a phantom, a closed loop pump-nozzle assembly with one inlet and two outlets (Fig. 3). The phantom simulates the far field flow of the fan organs which generate water jets preserving the amount of water involved in the motion. The fluid mass conservation is achieved by feeding the outlet nozzles with the fluid pumped from the sink via a closed loop. As in the case with live animals, an inflow appears to replace the fluid taken in by the sink (and then ejected as jets), and the fluid entrained by the jets. The phantom allows to generate horizontal sideward jets, jets directed 45° backwards, and jets directed 45° upwards and is manufactured in the size of a crayfish. Velocity of the flow induced by the mimicking device was measured with the same PIV arrangements used for the crayfish and the flow rate through the nozzles was adjusted to make the magnitude of the inflow close to that observed in experiments with live animals.

Results

A crayfish produced one or two jets by waving the fan organs of one or of either sides (Fig. 4). Jets' direction varied from 90° to the animal plane of symmetry to 45° upwards and 45° backwards. The jets of the length more than 10 cm were observed. Fanning was sometimes accompanied by flicking the antennules, a behaviour that enhances olfaction in decapod crustaceans (Schmitt and Ache, 1979). The animals may occasionally walk on the treadmill while waving the fan organs, but most of the time their walking legs are steady.

The outward jets induce an inflow converging towards the fan organs and the jets themselves. A typical flow field measured by PIV in the vertical

plain is shown in Fig. 5. The antennules are lowered in front of the fan organs thereby exposing olfactory receptors to the incoming flow. The streamlines in Fig. 5 are more or less horizontal at the level of fan organs which suggests that one can study the flow structure around the animal by measuring the flow field at this hight. Four examples of the flow field measured in the horizontal plane are shown in Fig. 6. The streamlines leading to the animal chemoreceptors illustrate that the sector of odour attraction may vary. The jets are out of the plane of measurement in most of experiments with live animals, which may create an illusion of breaking the fluid mass conservation. Four samples of the flow field generated by the mimicking device are shown in Fig. 8. The inflow patterns illustrate how the flow outside the jets converges towards the jets' origin (nozzles), and towards the jet axis.

A reasonable question to ask is how long does it take for the inflow pattern to adjust to the changed configuration of the jets. Since the animal's fanning behaviour is out of our direct control, we have performed experiments with the phantom. Several experimental runs with the flow through nozzles switched on from the rest showed that the steady flow field is set within several seconds after starting the pump.

The flow velocity as a function of distance from the fan organs/sink along the streamlines is plotted in Figs. 7 and 9. The slopes of the plots show that the flow velocity is somewhat inversely proportional to the distance from the fan organs i.e.

$$V \sim V_0 \frac{s_0}{s} \tag{1}$$

where V_0 is the fluid velocity at a distance s_0 from the fan organs. The time required for the odour patch located at a distance L from the fan organs to reach the crayfish antennules can be estimated by integrating inverse velocity by the distance:

$$T \sim \int_0^L \frac{1}{V}\, ds = \int_0^L \frac{1}{V_0}\frac{s}{s_0}\, ds = \frac{L^2}{2V_0 s_0} \tag{2}$$

Assuming the velocity $V_0 \approx 5$ mm/s at $s_0 = 10$ mm (as in Fig. 7) we can infer that the odour patch from stimulus located at 100 mm from the crayfish fan organs would reach the chemoreceptors in approximately 100 s. This time interval increases quadratically with L, rising to approximately 4 min for the distance of 150 mm. For comparison, solution of the diffusion equation for

the point source (Batchelor, 1970, p.187) shows that the characteristic time of molecular diffusion at a distance of 100 mm is measured in days.

Discussion

We have described a mechanism which crayfish may utilize to assess odour stimuli in a stagnant water environment. Using the anterior fan organs a crayfish creates jets (Fig. 4) so that the flow induced by these jets (Figs. 5, 6) draws a water sample from a distance to the animal's chemoreceptors. Schematic of the flow around the crayfish is sketched in Fig. 3.

The most important fact revealed by the PIV measurements is a surprisingly slow decrease of the inflow velocity with the distance from fan organs, the jets' origin (Figs. 7, 9). The slow decay is explained by the fluid entrainment by jets. If the entrainment was insignificant and the inflow was formed only by a point sink at the location of fan organs (the jets' origin), one would expect the inflow to be spherically symmetric (Batchelor, 1970, p.89). In that case the flow velocity would decrease as the inverse square of the distance from fan organs, and the travel time T for the odour patch to reach the crayfish chemoreceptors (equation 2) would be proportional to the 3rd power of the distance L to the odour source. This would increase the travel time to 10 min for a distance of 100 mm and to 40 min for a distance of 150 mm. Such time intervals are beyond the biologically relevant time scale. Note that, despite slow decrease with the distance, the inflow induced by jets is limited in space by the length of these jets as illustrated in Fig. 3a.

Fluid entrainment by a single jet has been described theoretically by Schneider (1981). He showed that a turbulent jet acts as a line sink with respect to the surrounding fluid. This leads to the axial rather than spherical symmetry of the flow field, hence to a slower decay of velocity with the distance. The decay is now proportional to inverse distance from the jet axis (a line) instead of inverse squared distance from the sink (a point). The secondary flow induced by a turbulent jet and decay of the jet itself were described analytically by Kotsovinos and Angelidis (1991). However, results of this paper can not be extended to a case of two jets because the Navier-Stokes equations governing fluid motion are not linear. Moreover, the relatively weak jets created by a crayfish can not be considered as fully developed turbulent jets, and presence of a rigid boundary, the bottom of the tank, affects the flow. The above argument suggests employment of direct

numerical simulation to model the flow induced by the jets, and the numerical simulation of a system of jets is a problem on its own. In this work, we do not go further in the investigation of a particular inflow structure, observing that the range of odour acquisition, i.e. the range where the inflow rate decreases slowly with the distance, is now defined by the jets' length which may exceed 10 cm.

To locate a source of the odour the crayfish needs to define a direction to this source. In a riverine environment the source is somewhere upstream. In still water an animal can navigate comparing the local intensity of the odour at different locations through the plume (Atema 1996). However, the animal movement may stir up the water and destroy the pattern of odour patches formed by the source. Active movement would also increase predation risks and may be energetically expensive. The crayfish can overcome these difficulties by scanning the environment employing a selection of jet patterns intended to provide varying directions of incoming flow as shown in Fig. 6, 8. Predation risks are now significantly reduced since hydrodynamic disturbance created by jets is detectable from a shorter distance in comparison with the moving visual target. When the bottom of a pond or a lake is covered by plants, scanning of environment with the help of jets becomes also energetically profitable since the stalks are less an obstacle to the flow than they are to the walking crayfish.

To show that production of the jets is not energetically expensive, we make an estimate based on parameters measured by Breithaupt (2001). Consider 6 appendages of the area $A = 10\,\mathrm{mm}^2$ each waving with the frequency $f = 6\,\mathrm{Hz}$, amplitude $a = 5\,\mathrm{mm}$, and velocity $u = 2\pi f a \approx 20\,\mathrm{cm/s}$. Water density is $\rho = 1000\,\mathrm{kg/m}^3$, its kinematic viscosity is $\nu = 0.01\,\mathrm{cm}^2/\mathrm{s}$. The Reynolds number of the flow around an appendage can be estimated as

$$\mathrm{Re} = \frac{u \cdot a}{\nu} = \frac{20\,\mathrm{cm\,s^{-1}} \cdot 0.5\,\mathrm{cm}}{0.01\,\mathrm{cm^2\,s^{-1}}} \approx 1000, \tag{3}$$

so that we can assume that the resistance force overcame by an appendage is defined by the dynamic term

$$F = \frac{1}{2}\rho u^2 \cdot A. \tag{4}$$

The energy required to wave the 6 appendages for a week is

$$E \approx 604800 \frac{\mathrm{s}}{\mathrm{week}} \cdot f \cdot 6\,\mathrm{appendages} \cdot F \cdot a \approx 20\,\mathrm{J} \approx 5\,\mathrm{Calories} \tag{5}$$

Allowing for the variability of the appendage area, the beat frequency, and the efficiency of the muscles driving the fan organs (10%) the estimated energy can rise to 200 Calories which is still small compared to the total energy gained by feeding in a week.

Observations of an unrestrained crayfish show that it may fan the appendages both when walking and when hiding in a shelter. This suggests that the animal creates the inflow both to assist active search for food and to detect the food appearance in the vicinity of the shelter. To understand the exact way in which the crayfish utilizes its self-generated inflow, behavioural experiments are required with unrestrained animals in a large tank.

Experiments with the phantom (Fig. 8) helped to understand the mechanism of odour attraction employed by the crayfish. This mechanism could well be adapted to design better robots for finding chemical sources in stagnant fluids. Nozzle assemblies generating one or several jets should be more efficient in drawing distant odour patches to the sensor than devices that create a sink flow. Unlike the live animals, a man-made mechanic assembly has fewer restrictions on the parameters affecting performance of the system. By optimizing nozzle profiles the jets can be made more regular and by increasing the pump power jets can be made considerably longer than those generated by a crayfish (up to metres). A number of jets and their alignment can be altered to obtain a desirable pattern of the inflow. Placing a set of sensors at different locations around the nozzles would enable measurement of the direction where the odour is coming from. Measurements of the time lag between switching the jets on and arrival of a chemical would add the data about the distance to the source.

The range of odour acquisition (the range of a relatively slow decrease of the inflow rate with the distance from the generating assembly) and the directional sensitivity of the robot is defined by the length of jets rather than by physical size of the device. This would allow design of a relatively small device with an ability to access the obstructed area of interest. Moreover, induction of the inflow by the outward jets would eliminate necessity of direct access to the area enabling, for example, chemical sensing through the mesh. Devices similar to that described above can be employed to search leaks from the pipes, to search chemical sources at the ocean bed, or for the non-invasive flow monitoring. The idea of using a jet to create an inflow is not restricted to the aquatic environment and can be used, for example, for the non-invasive monitoring of the agricultural land.

We would like to acknowledge financial support of this study by the Hull

Environmental Research Institute to T.B. and S.L. and a NERC fellowship NER/I/S/2000/01411 to T.B.

References

Atema, J. (1996) Eddy chemotaxis and odor landscapes: exploration of nature with animal sensors. *Biol. Bull.* **191**, 129–138.

Atema, J. (1985) Chemoreception in the sea: adaptations of chemoreceptors and behaviour to aquatic stimulus conditions. *Symp. Soc. Exp. Biol.* **39** (1985) 386–423.

Ayers, J. (2004) Underwater walking. *Arthropod. Struct. Dev.* **33**, 347–360.

Balkovsky, E., Shraiman, B.I. (2000) Olfactory search at high Reynolds number. *PNAS* **99(20)**, 12589–12593.

Batchelor, G.K. (1970) An introduction to Fluid Dynamics. *Cambridge University Press.*

Bergman, D.A., Martin, A.L. and Moore, P.A. (2005) Control of information flow through the influence of mechanical and chemical signals during agonistic encounters by the crayfish, *Orconectes rusticus. Animal Behaviour* **70**, 485–496.

Blackburn, N., Fenchel, T., and Mitchell, J. (1998) Microscale nutrient patches in planktonic habitats shown by chemotactic bacteria. *Science* **282**, 2254–2256.

Breithaupt, T. (2001) Fan organs of crayfish enhance chemical information flow. *Biol. Bull.* **200**, 150–154.

Breithaupt, T. and Eger, P. (2002) Urine makes the difference: chemical communication in fighting crayfish made visible. *J. Exp. Biol.* **205**, 1221–1231.

Brock, F. (1926) Das Verhalten des Einsiedlerkrebses Pagurus arrosor Herbst wahrend der Suche und Aufnahme der Nahrung. *Zeitschrift fur Morphologie und Okologie der Tiere* **6**, 415–552.

Budd, T.W., Lewis, J.C. and Tracey, M.L. (1979) Filtration feeding in Orconectes propinquus and Cambarus robustus (Decapoda, Cambaridae). *Crustaceana Supplement* **5**, 131–134.

Burrows, M. and Willows, A.O.D. (1969) Neuronal co-ordination of rhythmic maxilliped beating in brachyuran and anomuran crustacea. *Compar. Biochem. Phys.* **31**, 121–135.

Dusenbery, D.B. (1992) *Sensory Ecology.* New York: W.H.Freeman and Co.

Edwards, D.H., Jr. (1984) Crayfish extraretinal photoreception. I. Behavioral and motorneuronal responses to abdominal illumination. *J. Exp. Biol.* **109**, 291–306.

Grasso, F.W. (2001) Invertebrate-inspired sensory-motor systems and autonomous, olfactory-guided exploration. *Biol. Bull.* **200** 160–168.

Grasso, F.W., Basil, J.A. (2002) How lobsters, crayfishes, and crabs locate sources of odor: current perspectives and future directions. *Curr. Opin. Neurobiol.* **12**, 721–727.

Herberholz, J. and Schmitz, B. (2001) Signaling via Water Currents in Behavioral Interactions of Snapping Shrimp (Alpheus heterochaelis). *Biol. Bull.* **201**, 6–16.

Ishida, H., Tanaka, H., Taniguchi, H., Moriizumi, T. (2006) Mobile robot navigation using vision and olfaction to search for a gas/odor source. *Auton. Robot.* **20**, 231–238.

Kotsovinos, N.E. and Angelidis, P.B. (1991) The momentum flux in turbulent submerged jets. *J. Fluid Mech.* **229**, 453-470.

Martinez, D., Rochel, O., Hugues, E. (2006) A biomimetic robot for tracking specific odors in turbulent plumes. *Auton. Robot* **20**, 185–195.

Moore, P.A. and Grills, J.L. (1999) Chemical orientation to food by the crayfish Orconectes rusticus: influence of hydrodynamics. *Animal Behaviour* **58**, 953–963.

Sandeman, D.C., Sandeman, R.E., & de Couet, H.G. (1990) Extraretinal photoreceptors in the brain of the crayfish Cherax destructor. *J. Neurobiol.* **21**, 619–29.

Schmitt, B.C. & Ache, B.W. (1979) Olfaction: Responses of a decapod crustacean are enhanced by flicking. *Science*, **205**, 204–206.

Schneider, W (1981) Flow induced by jets and plumes. *J. Fluid Mech.* **108**, 55–65.

Vickers, N.J. (2000) Mechanisms of animal navigation in odor plumes. *Biol. Bull.* **198**, (2000) 203–212.

Weissburg, M.J. (2000) The Fluid Dynamical Context of Chemosensory Behavior. *Biol. Bull.* **198**, 188–202.

Weissburg, M.J. and Derby, C.D. (1995) Regulation of sex-specific feeding behavior in fiddler crabs: physiological properties of chemoreceptor neurons in claws and legs of males and females. *J. Compar. Phys. A* **176**, 513–526.

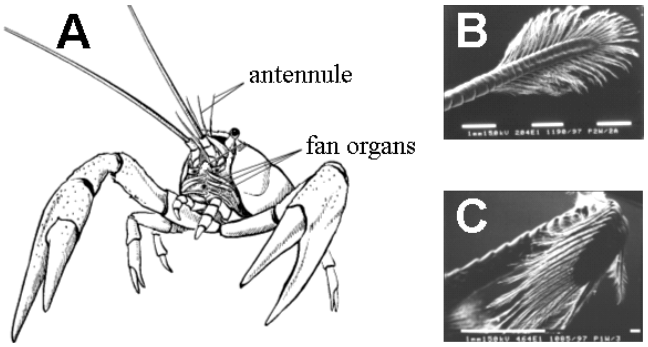


Figure 1: (A) Location of fan organs and major chemoreceptors (antennules) of crayfish. The fan organs are multisegmental flagellae (exopodite) of the mouthparts (maxilliped) and are feathered distally (B). During the power stroke (B; SEM picture) the feathered hairs are extended. During the recovery stroke (C; SEM picture) the feathered hairs are folded in. White bars in SEM pictures are to scale (1 mm). Reprinted from (Breithaupt, 2001) with permission of Biological Bulletin.

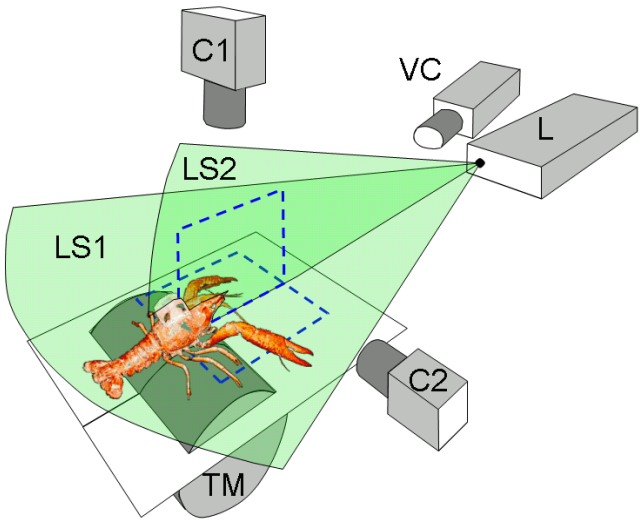


Figure 2: Experimental setup. A crayfish is suspended above the treadmill TM. A lasersheet is generated by a laser L. The PIV camera is set to the position C1(C2) and the lasersheet is aligned along the plane LS1(LS2) to measure the two components of velocity field in horizontal(vertical) planes. The video camera VC is used to monitor the crayfish fanning activity.

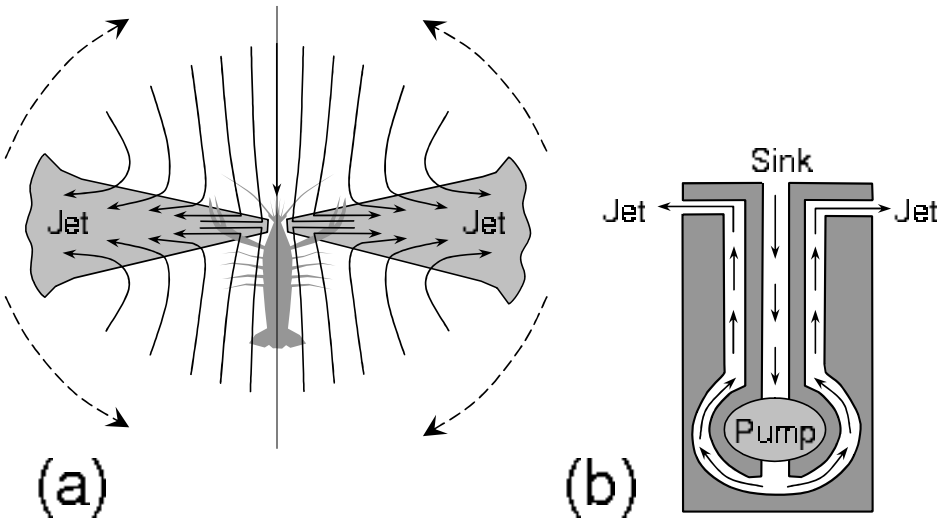


Figure 3: The flow generated by crayfish fan organs consists of the jets and the inflow (a). The inflow converges towards the jets' origin and towards jets' axes. At a distance larger than the jets' length the flow is virtually unaffected by a crayfish fanning activity. The jets are generally out of horizontal plane, so the sketch shows a projection. To mimic the flow created by a crayfish, an assembly of an inlet and two outlet nozzles (b) is designed. The water is pumped through a closed loop providing the fluid conservation which is obviously the case for a crayfish. Jets created by the animal are generally out of horizontal plane and thus are not presented in the measured flow fields.

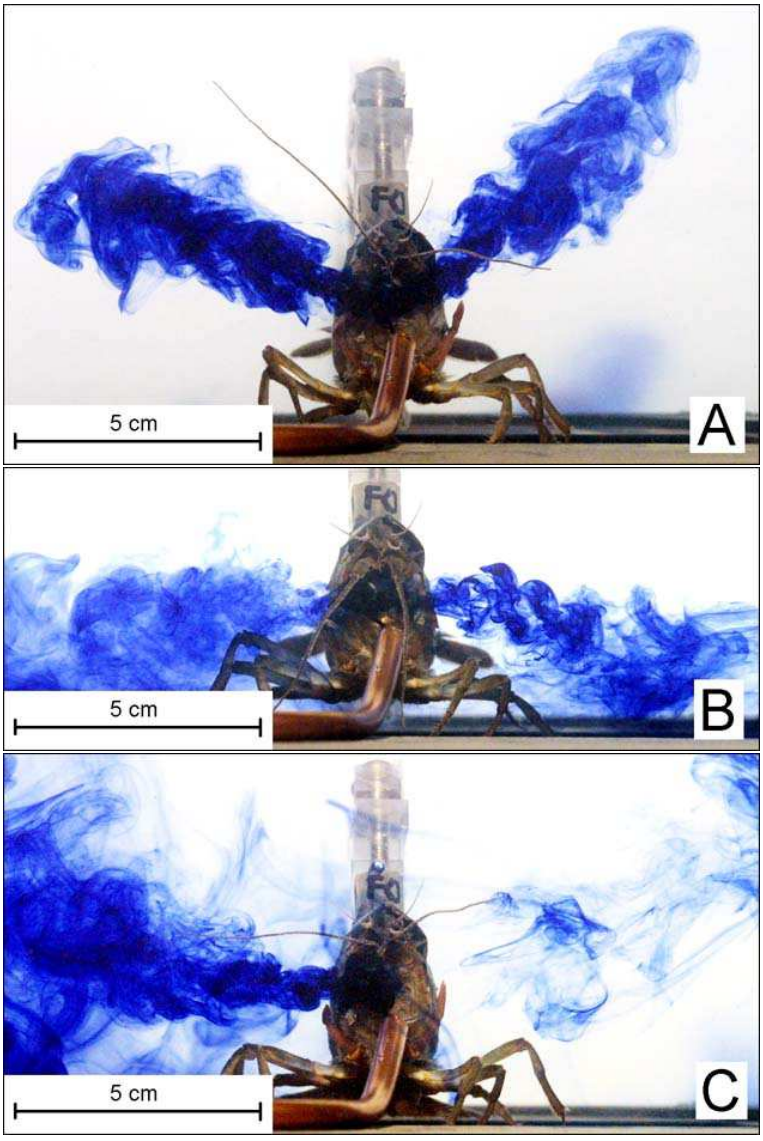


Figure 4: Ink visualization of the jets generated by the crayfish fan organs. Bilateral jets directed at 25° and 40° upwards (a) and horizontally (b); unilateral jet directed horizontally (c). The ink is slowly released from a pipe in front of the animal fan organs.

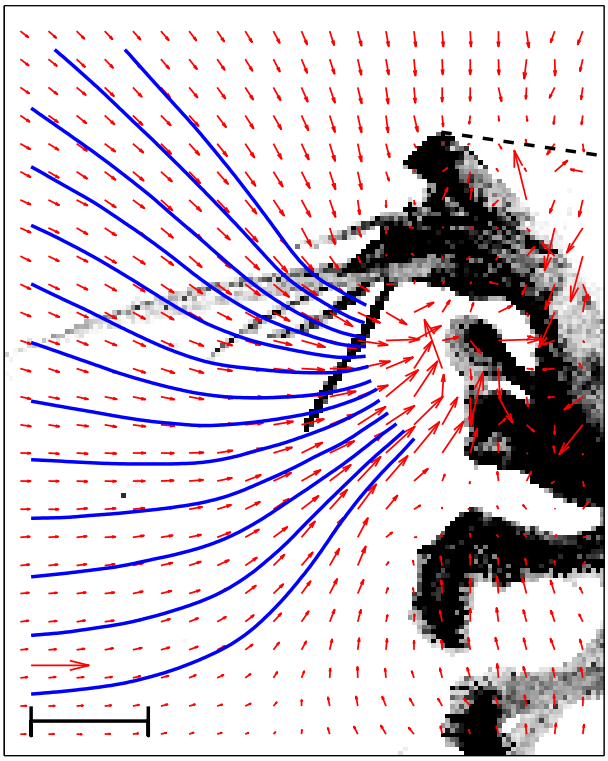


Figure 5: The flow field measured at the crayfish plane of symmetry (laser-sheet LS2 in Fig. 2). Average over 30 instantaneous measurements (30 seconds). A negative image of the crayfish cut from a PIV image is shown for reference. Observe that antennules with the chemoreceptors are lowered in front of fan organs. A reference vector at the bottom left is 1 cm/s, a reference segment is 1 cm.

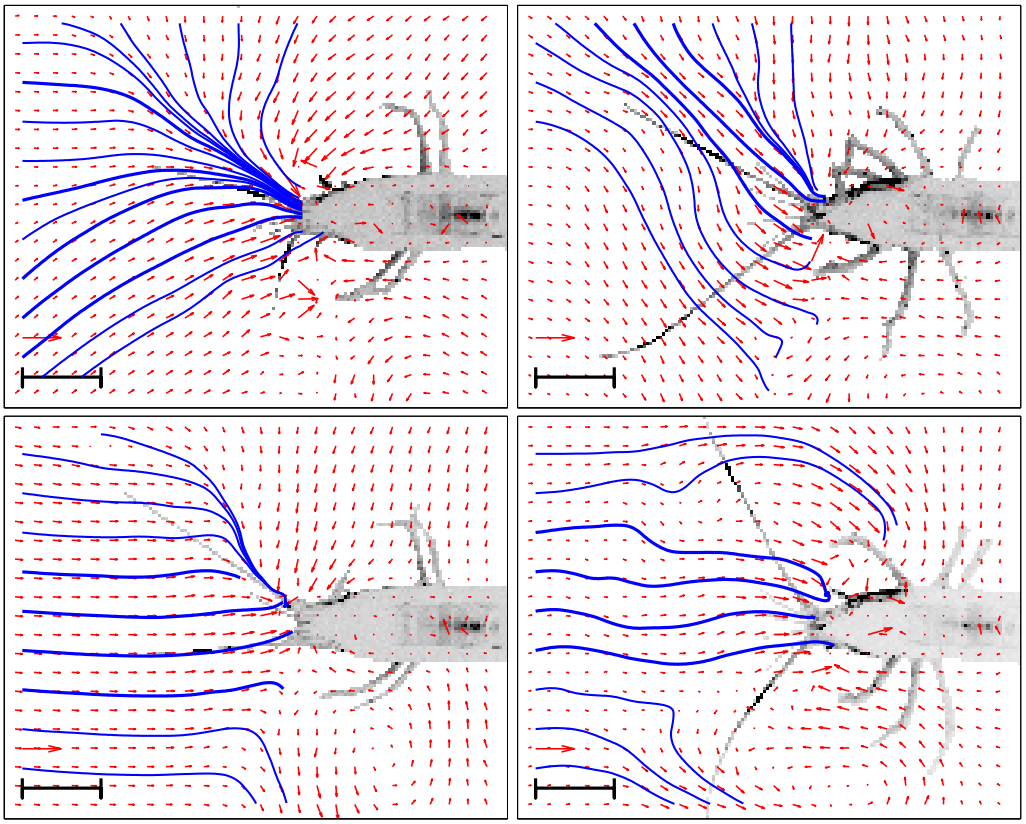


Figure 6: Velocity field generated by a crayfish measured in a horizontal plane LS1 (Fig. 2). Average over 30 instantaneous measurements (30 seconds). A negative image of the animal cut from a PIV image is shown for a reference. A reference vector at the bottom left is 1 cm/s, a reference segment is 2 cm. The jets created by the animal are outside the plane of measurement and thus are not observed in the vector field.

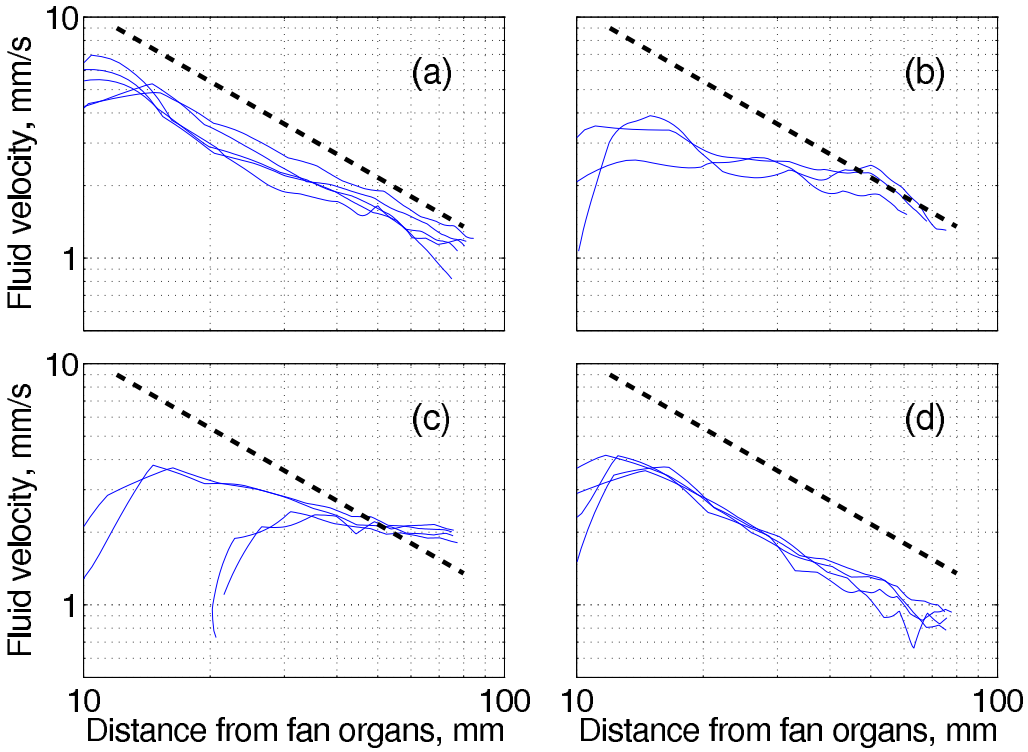


Figure 7: Absolute value of fluid velocity plotted *vs.* distance from the crayfish fan organs along the streamlines shown in bold in Fig. 6. The dashed lines correspond to $V \propto 1/s$ as in formula (1).

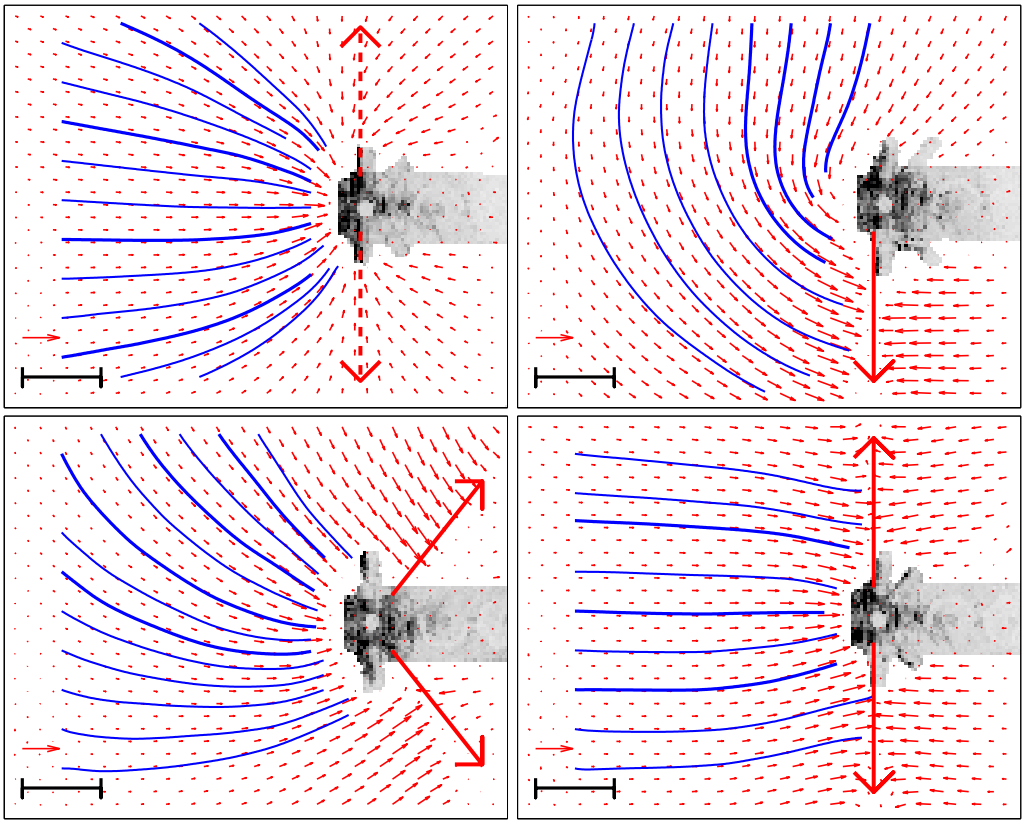


Figure 8: Velocity field generated by a mimicking device (Fig. 3b) measured in a horizontal plane LS1 (Fig. 2). A negative image of the device cut from a PIV image is shown for a reference. Positions of the jets produced by a model are indicated by bold lines. Two jets directed 45° upwards, off-plane (a), a single jet directed to the left (b), the two jets directed 45° backwards (c), and two jets directed to the sides (d). A reference vector at the bottom left is 1 cm/s, a reference segment is 2 cm. Short arrows at jet locations and over the model correspond to the 'noise' of image processing software and are not indicating any real values of fluid velocity.

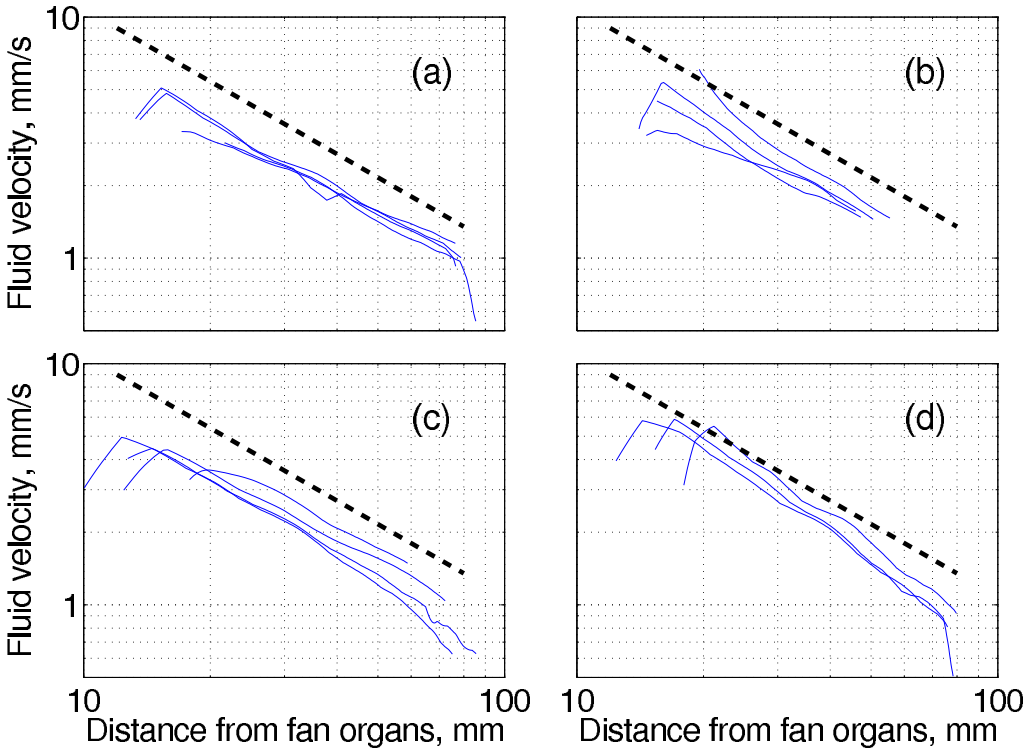


Figure 9: Absolute value of fluid velocity *vs.* distance from the jets origin along the streamlines shown in bold in Fig. 8. The dashed line line corresponds to $V \propto 1/s$ as in formula (1).